

## TOP QUARK PRODUCTION DYNAMICS IN QCD

EDMOND L. BERGER

High Energy Physics Division, Argonne National Laboratory, Argonne, IL 60439-4815, USA  
E-mail: ELB@hep.anl.gov

and

HARRY CONTOPANAGOS

High Energy Physics Division, Argonne National Laboratory, Argonne, IL 60439-4815, USA  
E-mail: CONTOPAN@hep.anl.gov

## ABSTRACT

A calculation of the total cross section for top quark production in hadron-hadron collisions is presented based on an all-orders perturbative resummation of initial-state gluon radiative contributions to the basic quantum chromodynamics subprocesses. Principal-value resummation is used to evaluate all relevant large threshold contributions. In this method there are no arbitrary infrared cut-offs, and the perturbative regime of applicability is well defined, two attributes that significantly reduce the estimated uncertainty of the results. For pp collisions at center-of-mass energy  $\sqrt{s} = 1.8$  TeV and a top mass of 175 GeV, we obtain  $\sigma(tt) = 5.52^{+0.07}_{-0.45}$  pb, in agreement with experiment. Predicted cross sections are provided as a function of top mass in pp collisions at  $\sqrt{s} = 2.0$  TeV and in pp collisions at CERN LHC energies.

## 1. Introduction

The quest for the top quark  $t$  reached fruition in the past year with the observation of  $tt$  pair production in proton-antiproton collisions at the Fermilab Tevatron<sup>1</sup>. A deserving question is the quantitative reliability of theoretical computations of the total cross section, as a function of top mass, based on the main production mechanisms in perturbative quantum chromodynamics (pQCD). In this paper, we discuss the motivation for incorporating the effects of initial-state gluon radiative corrections, and we present our all-orders resummation of these contributions.<sup>2</sup>

At lowest order in perturbation theory, two QCD partonic subprocesses contribute to  $p + p \rightarrow t + t + X$ . They are quark-antiquark annihilation:  $q + \bar{q} \rightarrow t + t$  and

---

Invited paper presented by E. L. Berger at the International Symposium on Heavy Flavor and Electroweak Theory, Beijing, August 16 - 19, 1995

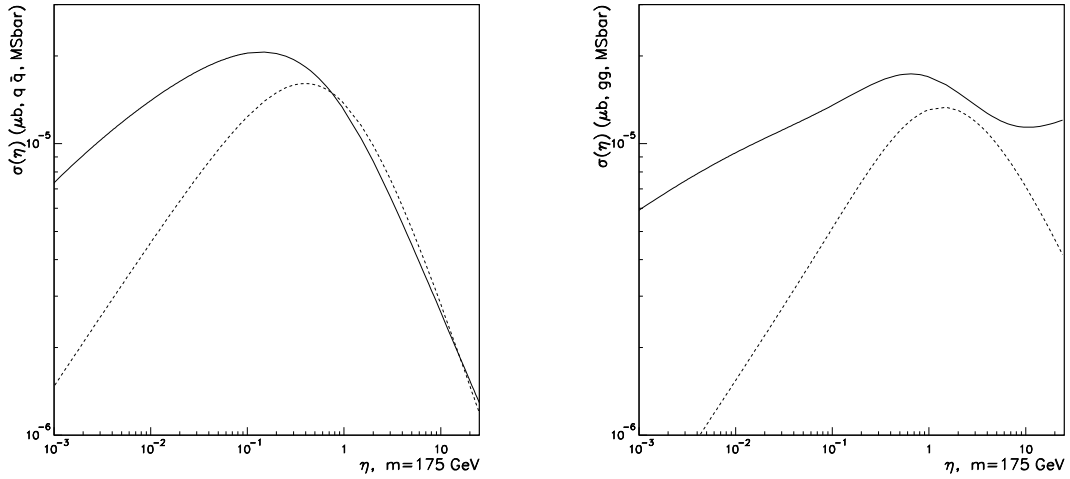


Fig. 1. The parton-parton cross sections as a function of  $\eta$  in the  $\overline{\text{MS}}$  scheme at  $m = 175$  GeV for the subprocesses (a)  $qq \rightarrow ttX$  and (b)  $gg \rightarrow ttX$ . Plotted are the lowest order Born cross section (dotted line) and the next-to-leading order cross section (solid line). The QCD scale  $\mu = m$ .

gluon-gluon fusion:  $g + g \rightarrow t + t$ . Short-distance partonic cross sections based on these lowest order  $\mathcal{O}(\frac{2}{s})$  subprocesses and on the next-to-leading  $\mathcal{O}(\frac{3}{s})$  subprocesses have been investigated thoroughly.<sup>3,4</sup> A full  $\mathcal{O}(\frac{n}{s})$  calculation, for  $n \geq 4$ , does not exist. The physical top quark cross section is obtained from a convolution of the perturbative short-distance subprocess cross sections with parton distributions that specify the probability densities of the quarks, antiquarks, and gluons of the incident  $p$  and  $p$ . Our work addresses improvements in the reliability of calculations of the subprocess cross sections.

The motivation for this work begins with the observation that the size of the  $\mathcal{O}(\frac{3}{s})$  terms in the  $qq$  and  $gg$  partonic cross sections are much larger than their  $\mathcal{O}(\frac{2}{s})$  counterparts in some kinematic regions, notably in the near-threshold region of small  $\eta$ . The variable  $\eta = \hat{s} - 4m^2$ , where  $\hat{s}$  is the square of the energy of parton-parton subprocess and  $m$  denotes the mass of the top quark. Variable  $\eta$  measures the "distance" above the partonic production threshold.

As shown in Fig. 1, for a top mass of 175 GeV, in both the  $qq$  and the  $gg$  channels the size of the  $\mathcal{O}(\frac{3}{s})$  term exceeds that of the  $\mathcal{O}(\frac{2}{s})$  term for  $\eta < 0.1$ , and the ratio grows as  $\eta$  decreases.<sup>2</sup> Therefore, the important notion underlying perturbation theory, that successive terms in the perturbation series should be smaller, is not valid at small  $\eta$ , i.e., in the region near production threshold. This region of phase space is important for top quark production at the Tevatron. Owing to the large mass of the top quark, relative to the  $pp$  center of mass energy  $\sqrt{s}$ , the near-threshold region

contributes significantly when the convolution integral, mentioned above, is done over the full range of  $\beta$ . Consistency in the results of a perturbative calculation of the overall  $t\bar{t}$  cross section requires an appropriate understanding of the origin of the large next-to-leading order enhancement of the partonic cross sections near threshold. (In the  $gg$  channel, the ratio of the  $O(\beta^3)$  and  $O(\beta^2)$  terms exceeds unity for large  $\beta$  also. The  $gg$  channel and the large  $\beta$  region are important for bottom quark production at the Tevatron<sup>5</sup>, but not for top quark production.)

We treat only  $t\bar{t}$  pair production. Mechanisms for single top production<sup>6</sup> are not considered here. At  $m = 175 \text{ GeV}$  and  $\sqrt{s} = 1.8 \text{ TeV}$ , they contribute a cross section about 20% that of the pair production mechanisms.

## 2. Gluon Radiation and Resummation

The origin of the large threshold enhancements in the subprocess cross sections may be traced to initial-state gluon radiation.<sup>3</sup> After the cancellation of soft singularities between the contributions from real gluon emission and virtual gluon exchange terms, and proper factorization of collinear divergences, there remain terms at  $O(\beta^3)$  that are proportional to  $\ln(1-z)$ . The variable  $z = 1 - 2k_g \cdot p_t / m^2$  where  $p_t$  and  $k_g$  are the four-momenta of the produced top quark and the gluon radiated into the final state in the  $2 \rightarrow 3$  process. The limit  $z \rightarrow 1$  corresponds to zero momentum carried by the gluon.

The partonic cross section may be expressed generally as

$$\hat{\sigma}_{ij}(\beta; m^2) = \int_{z_{\text{min}}}^{z=1} dz [1 + H_{ij}(z; \beta)] \hat{\sigma}_{ij}^{(0)}(\beta; m^2; z) \quad (1)$$

In the near threshold region,

$$H_{ij}(z; \beta) \approx 2 C_{ij} \ln^2(1-z) + \beta^2 2C_{ij}^2 \ln^4(1-z) + \frac{4}{3} C_{ij} b_2 \ln^3(1-z) \quad (2)$$

We work in the  $\overline{\text{MS}}$  factorization scheme in which the  $q$ ,  $\bar{q}$  and  $g$  densities and the next-to-leading order partonic cross sections are defined unambiguously. In Eq. (1), the lower limit of integration  $z_{\text{min}} = 1 - 4(1 + \beta^2) / 4(1 + \beta^2)$ , and  $ij \in \{qq, q\bar{q}, gq, gg\}$  denotes the initial parton channel. We set  $\sigma_s(m) = \dots$ . Symbol  $\hat{\sigma}_{ij}^{(0)}(\beta; m^2; z) = d(\hat{\sigma}_{ij}^{(0)}(\beta; m^2; z)) = dz$ , where  $\hat{\sigma}_{ij}^{(0)}$  is the lowest order partonic cross section expressed in terms of inelastic kinematic variables<sup>7</sup> to account for the emitted radiation. The integration in Eq. (1) is over the phase space of the radiated gluons, parametrized through the dimensionless variable  $z$ . In Eq. (2),  $C_{ij}$  is the color factor for the  $ij$  production channel.

Equation (2) approximates the near-threshold behavior of the partonic cross section. It manifests the logarithmic behavior  $\ln(1-z)$  mentioned above. Explicit calculations<sup>3</sup> of the complete  $O(\beta^3)$  cross section provide the  $2 C_{ij} \ln^2(1-z)$  term.



estimated uncertainties.

### 3. Principal Value Resummation

The principal-value method of resummation (PVR)<sup>9</sup> has an important technical advantage in that it does not depend on arbitrary infrared cut-offs, as all Landau-pole singularities are by-passed by a Cauchy principal-value prescription. Because extra undetermined scales are absent, the method also permits an evaluation of the perturbative regime of applicability of the method, i.e., the region of the gluon radiation phase space where perturbation theory should be valid. The method has been tested successfully in massive lepton-pair production.<sup>10</sup>

To illustrate how infrared cut-offs are avoided in the PVR method, it is useful to express in momentum space the exponent that resums the  $\ln(1-z)$  terms:

$$E(n; m^2) = \int_0^1 dx \frac{x^{n-1}}{1-x} \frac{d}{d\ln m^2} g^h : \quad (6)$$

The function  $g(\ln m^2)$  is calculable perturbatively, but, again, the behavior of  $g(\ln m^2)$  leads to divergence of the integral when  $m^2 \rightarrow Q_{CD}^2$ . To tame the divergence, a cut-off can be introduced in the integral over  $x$  or directly in momentum space, in the fashion of Laenen et al.<sup>7</sup> In the principal-value redefinition of resummation, the singularity is avoided by replacement of the integral over the real axis  $x$  in Eq. (6) by an integral along a contour  $P$  in the complex plane:

$$E^{PV}(n; m^2) = \int_P \frac{z^{n-1}}{1-z} \frac{d}{d\ln m^2} g^h : \quad (7)$$

The function  $E^{PV}(n; m^2)$  is finite since the Landau pole singularity is by-passed. In Eq. (7), all large soft-gluon threshold contributions are included through the two-loop running of  $\alpha_s$ .

Equations (6) and (7) have identical perturbative content, but, when expanded in power series in  $(\ln m^2)$  and in  $Q_{CD} = m$ , they manifest differences in their inverse power (high-twist) terms. Since the inverse power content is not a prediction of perturbative QCD, neither expression is a priori preferable, except for the attractive finiteness of Eq. (7). In our application of principal-value resummation to top quark production, we choose to use the result only in the region of phase space in which the perturbative content dominates. Thus, the high-twist content of Eq. (7), and the difference between the high-twist components of Eqs. (7) and (6), are not matters of phenomenological significance.

After inversion of the Mellin transform, the resummed partonic cross sections according to PVR, including all large threshold corrections, can be written in the

form of Eq. (1), but with Eq. (2) replaced by

$$H_{ij}^{PV}(z; ) = \int_0^{\ln(\frac{1}{1-z})} dx e^{E_{ij}(x; )} \sum_{j=0}^{\infty} Q_j(x; ) : \quad (8)$$

The leading large threshold corrections are contained in the exponent  $E_{ij}(x; )$ , a calculable polynomial in  $x$ . The functions  $fQ_j(x; )g$  arise from the analytical inversion of the Mellin transform from momentum space to the physically relevant momentum space expressed in Eq. (8). These functions are produced by the resummation and are expressed in terms of successive derivatives of  $E : P_k(x; ) = \partial^k E(x; ) = k! \partial^k x$ .

The functional form of  $E_{ij}$  for tt production is identical to that for ll production, except for the identification of the two separate channels, denoted by the subscript  $ij$ . However, only the leading threshold corrections are universal. Final-state gluon radiation as well as initial-state/ nal-state interference e ects produce sub-leading logarithmic contributions that differ for processes with different nal states. Among all  $fQ_jg$  in Eq. (8), only the very leading one is universal. This is the linear term in  $P_1$ , which turns out to be  $P_1$  itself. Since we intend to resum only the universal leading logarithms, we retain only  $P_1$ . Hence, Eq. (8) can be integrated explicitly, and the resummed version of Eq. (1) is

$$\hat{H}_{ij}^{PV}(\hat{s}; m^2) = \int_{z_{min}}^{z_{max}} dz e^{E_{ij}(\ln(\frac{1}{1-z}); )} \hat{H}_{ij}^0(\hat{s}; m^2; z) : \quad (9)$$

The upper limit of integration in Eq. (9) is set by the boundary between the perturbative and high-twist regions. To characterize a region in momentum space as high-twist, one must convert to momentum space through inversion of the Mellin transform, Eq. (8). Specification of the boundary is realized by the constraint that all  $fQ_jg; j \geq 1$  be small compared to  $Q_0$ . This constraint can be shown to correspond to

$$P_1 \ln \frac{1}{1-z} ; < 1 : \quad (10)$$

As remarked above, we accept only the perturbative content of principal-value resummation, and our cross section is evaluated accordingly. Specially, we use Eq. (9) with the upper limit of integration,  $z_{max}$ , calculated from Eq. (10). The upshot is an effective threshold cut on the integral over the scaled subenergy variable  $z$ , reminiscent of that introduced by Laenen et al, but one that is calculable, not arbitrary. In our case, the cut restricts the region of applicability of resummation to the part of phase space in which the perturbative content of Eq. (8) is the dominant content. For the top mass  $m = 175$  GeV, we determine that the perturbative regime is restricted to  $z < 0.007$  for the  $qq$  channel and  $z < 0.05$  for the  $gg$  channel. The difference reflects the larger color factor in the  $gg$  case. (One could attempt to apply Eq. (9) all the way to  $z_{max} = 1$ , i.e., to  $z = 0$ , beyond the perturbative regime of Eq. (10), but one would then be using a model for non-perturbative e ects, the one suggested by PVR, far beyond the knowledge justified by perturbation theory.)

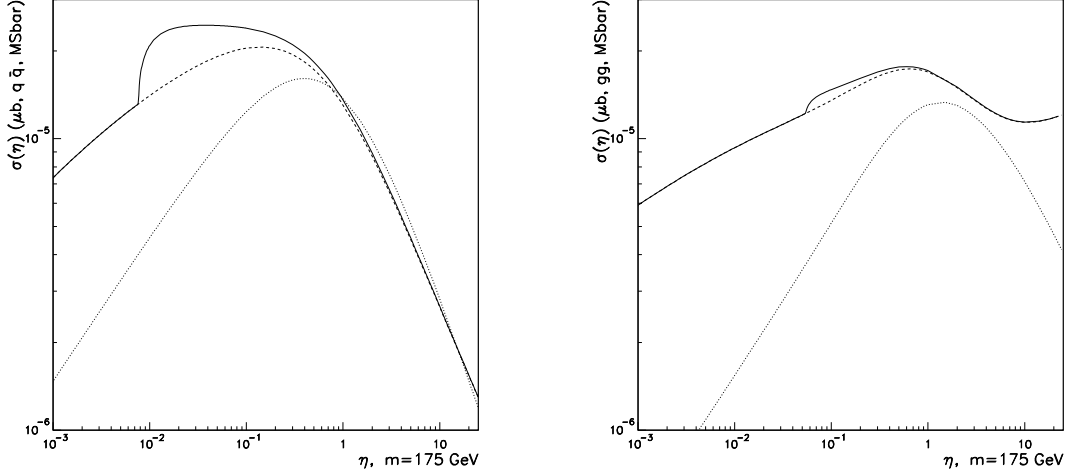


Fig. 2. The parton-parton cross sections as a function of  $\eta$  in the  $\overline{\text{MS}}$  scheme at  $m = 175$  GeV for the subprocesses (a)  $qq \rightarrow t\bar{t}X$  and (b)  $gg \rightarrow t\bar{t}X$ . Plotted are the lowest order Born cross section (dotted line), the next-to-leading order cross section (dashed line), and the resummed cross section (solid line). The QCD scale  $\mu = m$ .

Our final result does not rely critically on the PVR method to by-pass infrared renormalons and associated problems, precisely because we restrict application to the perturbative regime. In this regard, the presence of arbitrary infrared cuts in other resummation methods is superfluous, as all necessary information about infrared sensitivity (i.e., the perturbative regime) can be obtained by examining the perturbative asymptotic properties of the resummation functions.

The resummation procedure includes only the leading threshold  $\ln^2(1-z)$  piece of the full  $\mathcal{O}(\alpha_s^3)$  calculation. To restore the full content of the complete next-to-leading order calculation,  $\hat{\sigma}_{ij}^{(0+1)}$ , we define our final resummed cross sections for each production channel through the improved prediction

$$\hat{\sigma}_{ij}^{\text{nal}}(\eta; m^2) = \hat{\sigma}_{ij}^{\text{PVpert}}(\eta; m^2) + \hat{\sigma}_{ij}^{(0+1)}(\eta; m^2) - \hat{\sigma}_{ij}^{\text{PV}}(\eta; m^2) \quad (11)$$

The last term in Eq. (11) is the part of the next-to-leading order partonic cross section included in the resummation. In Fig 2 we present the resummed partonic cross sections in the  $qq$  and  $gg$  channels at  $m = 175$  GeV. We also show the lowest order and next-to-leading order counterparts. The three curves differ substantially in the partonic threshold region  $\eta < 1$ , with the final resummed curve exceeding the other two. Below  $\eta' = 0.007$  in the  $qq$  channel and  $\eta' = 0.05$  in the  $gg$  channel, our resummed cross sections become identical to the next-to-leading order cross sections, a consequence of our decision to restrict the resummation to the perturbative domain. Above

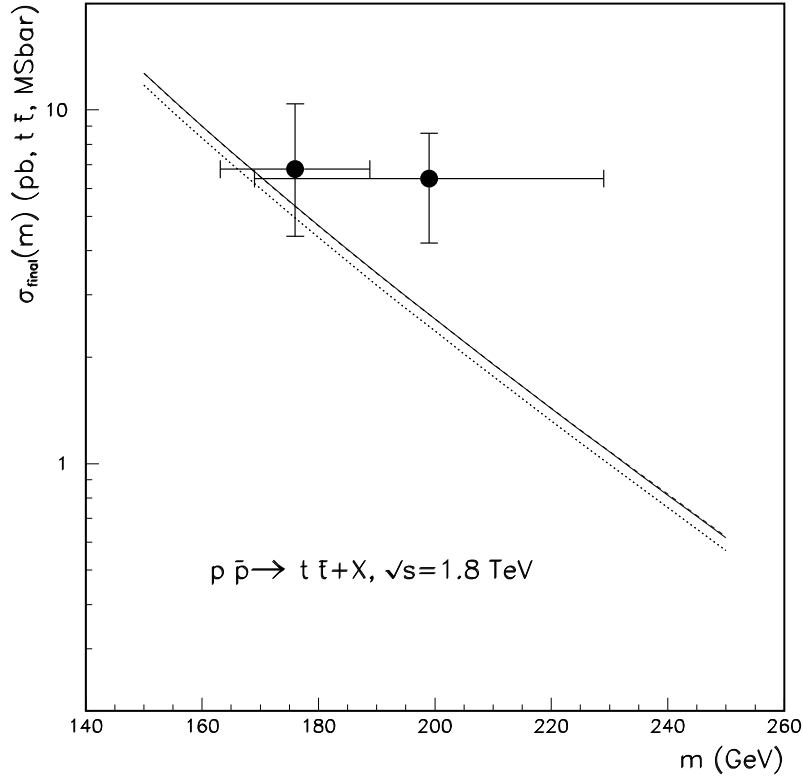


Fig. 3. Physical cross section for  $pp \rightarrow (t\bar{t})X$  at  $\sqrt{s} = 1.8$  TeV as a function of top mass. Data from the CDF and D0 collaborations<sup>1</sup> are plotted. Shown are calculations for three choices of the scale  $\mu = m = 0.5$  (dashed), 1 (solid), and 2 (dotted).

1, our resummed cross sections are essentially identical to the next-to-leading order cross sections, as is to be expected since the near-threshold enhancements that concern us in this paper are not relevant at large  $m$ .

#### 4. Calculations at $\sqrt{s} = 1.8$ TeV and $\sqrt{s} = 2$ TeV

In the remainder of this report, we present our results for the physical inclusive total cross section for  $t\bar{t}$  production for a top-mass range  $m \in [150; 250]$  GeV, including a discussion of the remaining theoretical uncertainties. We obtain the physical cross section by convoluting Eq. (11) with CTEQ3M parton densities<sup>11</sup> and adding the results from both channels. In Fig. 3 we show the top-mass dependence of the physical cross section for  $pp \rightarrow (t\bar{t})X$  at  $\sqrt{s} = 1.8$  TeV.

As illustrated in Fig. 4, the behavior of the physical cross section as a function of the renormalization/factorization scale is mild in the range  $\mu \in [0.5; 2]m$ . (The next-to-leading order result in Fig. 4 differs somewhat from that shown in our published paper.<sup>2</sup> Owing to a compiler error, the next-to-leading order curve in

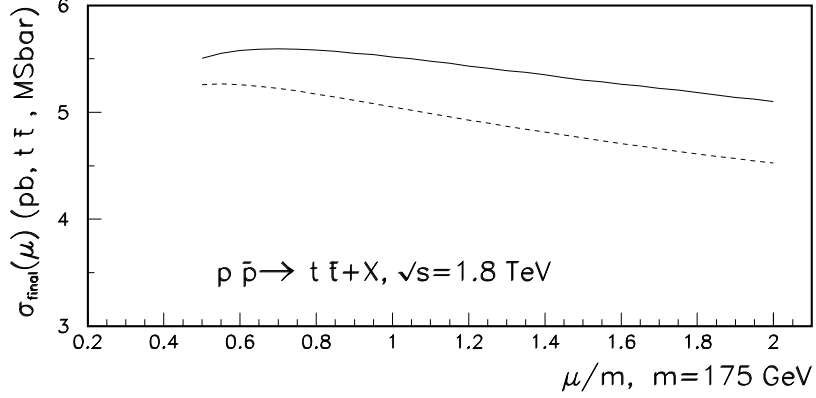


Fig. 4. Plot showing the calculated dependence of the final resummed cross section on  $(\mu/m)$  for  $t\bar{t}$  production at  $m = 175$  GeV and  $\sqrt{s} = 1.8$  TeV. Shown also is the next-to-leading order result (dashed curve).

the published figure is incorrect.) We consider the variation of the cross section in the range  $\mu/m \in [0.5; 2]$  to be a reasonable measure of the theoretical perturbative uncertainty. Over this range, the band of variation of the strong coupling strength  $\alpha_s$  is a generous 10%. We determine

$$\sigma^{t\bar{t}}(m = 175 \text{ GeV}; \sqrt{s} = 1.8 \text{ TeV}) = 5.52^{+0.07}_{-0.45} \text{ pb} : \quad (12)$$

We define the central value (5.52 pb) to be that obtained with  $\mu/m = 1$ . The upper and lower limits correspond to the maximum and minimum values of the cross section in the range  $\mu/m \in [0.5; 2]$ . The cross section is insensitive to the choice of parton densities. Repeating the same analysis with the MR S(A<sup>0</sup>) densities<sup>12</sup>, we obtain

$$\sigma^{t\bar{t}}(m = 175 \text{ GeV}; \sqrt{s} = 1.8 \text{ TeV}) = 5.32^{+0.08}_{-0.41} \text{ pb} : \quad (13)$$

The central values in Eqs. (12) and (13) are about 10% larger than that of Laenen et al., Eq. (5), but within the quoted uncertainties. Our calculated cross sections fall within the current uncertainty bands of the CDF and D0 experiments.<sup>1</sup>

The bands of perturbative uncertainty quoted in Eqs. (12) and (13) are relatively narrow. On the other hand, we noted in discussing Eq. (9) that  $z_{\text{max}} < 1$ , meaning that there is a reasonable range of  $\mu$  near threshold in which perturbative resummation does not apply. Perturbation theory is not justified in this region. Correspondingly, further strong interaction enhancements of the  $t\bar{t}$  cross section may arise from physics in this region. We know of no reliable way to estimate the size of such non-perturbative effects and, therefore, cannot include such uncertainties in the estimates of the perturbative uncertainty of Eqs. (12) and (13).

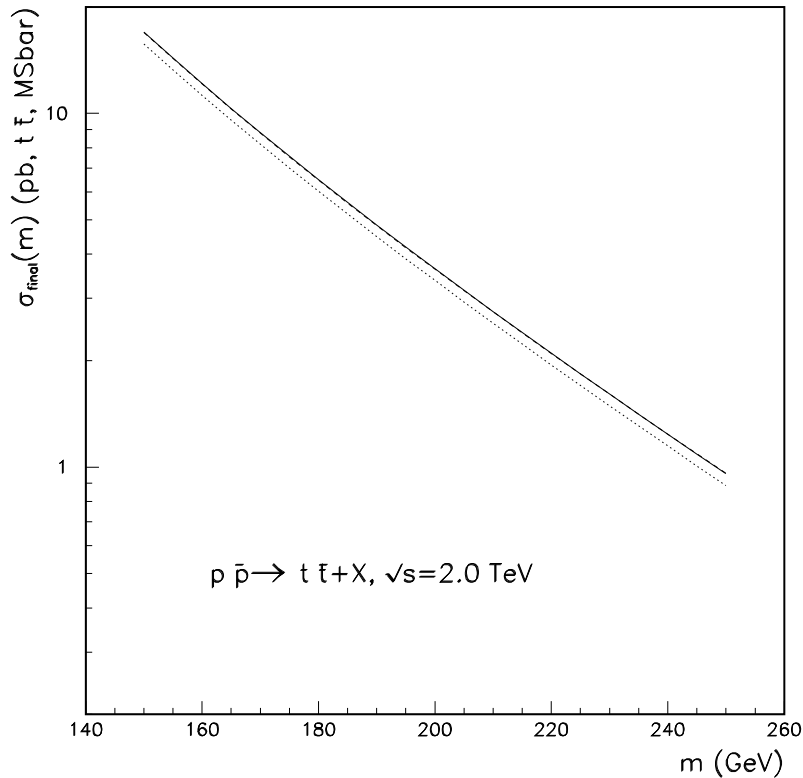


Fig. 5. Physical cross section for  $pp \rightarrow (t\bar{t})X$  at  $\sqrt{s} = 2 \text{ TeV}$  as a function of top  $m$  ass. Shown are calculations for three choices of the scale  $\mu = m = 0.5$  (dashed), 1 (solid), and 2 (dotted).

In Fig. 5 we show the top- $m$  ass dependence of the physical cross section for  $pp \rightarrow (t\bar{t})X$  at the slightly larger energy  $\sqrt{s} = 2 \text{ TeV}$ . We predict

$$\sigma^{tt}(m = 175 \text{ GeV}; \sqrt{s} = 2 \text{ TeV}) = 7.56^{+0.10}_{-0.55} \text{ pb} : \quad (14)$$

At  $m = 175 \text{ GeV}$ , the value of the cross section at  $\sqrt{s} = 2 \text{ TeV}$  is about 37% greater than that at  $\sqrt{s} = 1.8 \text{ TeV}$ .

## 5. LHC Predictions

Turning to  $pp$  scattering at the energies of the Large Hadron Collider (LHC) at CERN, we note a few significant differences from  $pp$  scattering at the energy of the Fermilab Tevatron. The dominance of the  $q\bar{q}$  production channel at the Tevatron is replaced by  $gg$  dominance at the LHC. Owing to the much larger value of  $\sqrt{s}$ , the near-threshold region in the subenergy variable is relatively less important, reducing the significance of initial-state soft gluon radiation. Lastly, physics in the region of large  $\sqrt{s}$ , where straightforward next-to-leading order QCD is also inadequate, may become significant for  $t\bar{t}$  production at LHC energies. Using the approach described in this paper, focussed on the resummation of initial-state gluon radiation, we present

predictions in Fig. 6 for LHC energies of 10 and 14 TeV. We estimate

$$\sigma_{\text{final}}^{t\bar{t}}(m = 175 \text{ GeV}; \sqrt{s} = 14 \text{ TeV}) = 760 \text{ pb} : \quad (15)$$

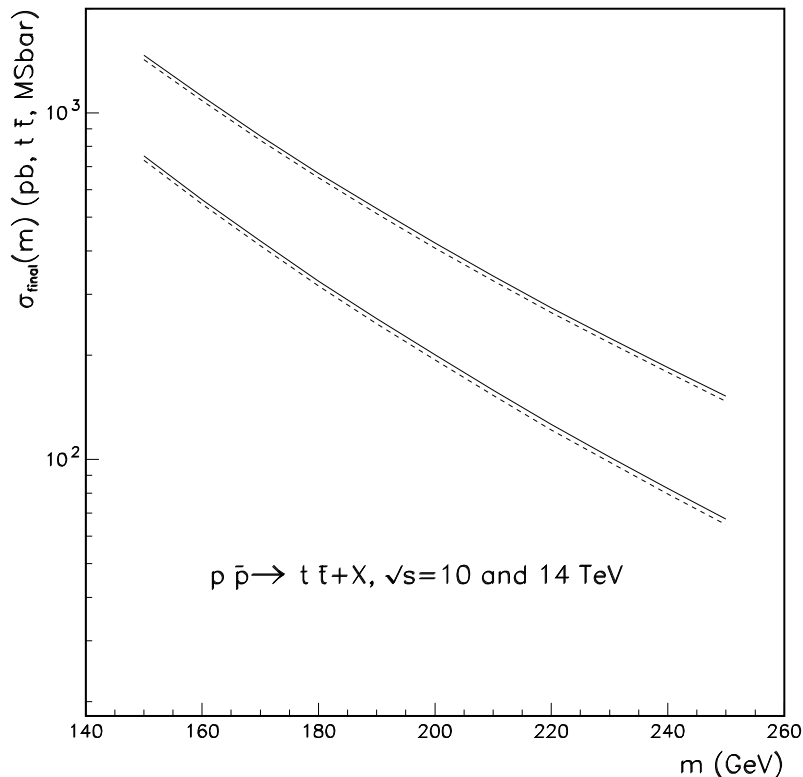


Fig. 6. Cross section for  $pp \rightarrow (t\bar{t})X$  at  $\sqrt{s} = 10$  and 14 TeV as a function of top mass. Shown are the next-to-leading order (dashed) and resummed (solid) calculations for the scale choice  $\mu = m$ .

## 6. Summary and Discussion

In summary, we present a calculation of the total cross section for  $t\bar{t}$  pair production in perturbative QCD including resummation of initial-state gluon radiation to all orders in  $\alpha_s$ . Two advantages of the principal-value method of resummation are the well-defined perturbative domain of applicability and the absence of arbitrary infrared cut-offs. Both  $q\bar{q}$  and  $g\bar{g}$  production channels are included in the calculation. At  $\sqrt{s} = 1.8$  TeV, our final resummed cross section is approximately 10% greater than the pure next-to-leading order result and in agreement with data. We provide predictions for the cross section as a function of top mass at  $\sqrt{s} = 2, 10, \text{ and } 14$  TeV.

We remark that the resummation method developed here and applied to  $t\bar{t}$  pair production is relevant in other situations in which dynamics probes the near-threshold

region in the scaled subenergy variable. An example of current interest at  $\sqrt{s} = 1.8$  TeV is the production of hadronic jets that carry large transverse momentum.<sup>13</sup>

## 7. Acknowledgements

ELB is pleased to acknowledge valuable comments from Stanley Brodsky and John Ellis, and he is grateful to Chao-Hsi Chang and Tau Huang for their warm hospitality in Beijing. This work was supported by the U.S. Department of Energy, Division of High Energy Physics, contract W-31-109-Eng-38.

## 8. References

1. F. Abe et al., Phys. Rev. Lett. 74 (1995) 2626; S. Abachi et al., Phys. Rev. Lett. 74 (1995) 2632.
2. E. Berger and H. Contopanagos, Phys. Lett. B 361 (1995) 115; Argonne report ANL-PR-95-82, to be published.
3. P. Nason, S. Dawson and R. K. Ellis, Nucl. Phys. B 303 (1988) 607; B 327 (1989) 49; Erratum: B 335 (1990) 260; W. Beenakker, H. Kuijf, W. L. van Neerven and J. Smith, Phys. Rev. D 40 (1989) 54; W. Beenakker, W. L. van Neerven, R. Meng, G. A. Schuler and J. Smith, Nucl. Phys. B 351 (1991) 507.
4. E. L. Berger and R. Meng, Phys. Rev. D 49 (1994) 3248, and references therein.
5. J. Collins and R. K. Ellis, Nucl. Phys. B 360 (1991) 3.
6. S. Willenbrock and D. Dicus, Phys. Rev. D 34 (1986) 155; C.-P. Yuan, Phys. Rev. D 41 (1990) 42; T. Stelzer and S. Willenbrock, Phys. Lett. 357B (1995) 125.
7. E. Laenen, J. Smith and W. L. van Neerven, Nucl. Phys. B 369 (1992) 543; Phys. Lett. 321B (1994) 254.
8. G. Sterman, Nucl. Phys. B 281 (1987) 310; S. Catani and L. Trentadue, Nucl. Phys. B 327 (1989) 323; B 353 (1991) 183; D. Appell, P. Mackenzie, and G. Sterman, Nucl. Phys. B 309 (1988) 259.
9. H. Contopanagos and G. Sterman, Nucl. Phys. B 400 (1993) 211; Nucl. Phys. B 419 (1994) 77.
10. L. A. Ivero and H. Contopanagos, ANL-HEP-PR-94-59/IITP-SB-94-41, Nucl. Phys. B (revised, in print).
11. H. L. Lai et al., Phys. Rev. D 51 (1995) 4763.
12. A. Martin, R. Roberts and W. J. Stirling, Phys. Lett. B 354 (1995) 155.
13. CDF Collaboration, A. Bhatti et al., Fermilab report FNAL-CONF-95/109-E.